Feasible Management of Non-degradable Agricultural Mulching Film Wastes into Functional Flame-retarded Materials

Wenfan Yu,[a,b] Xiangsheng Han,[a,b] Hongzhen Cai,[a,b] Wenyu Lu,[a,b] Hang Xu,[a,b] and Weiming Yi [a,b,*]

A feasible procedure was proposed to convert agriculture mulching film wastes into functional flame-retarded cotton stalk particles-polyethylene-sandy soil composites (CS-PE-SS_x) by simple compounding and injection molding. Due to the uniform dispersion of solid particles in polymer matrix and the promising interfacial combination and the potential interacting forces between cotton stalk and sandy soil particles, the resultant composites showed promising mechanical strength (a flexural strength of approximately 29.0 MPa, a tensile strength of approximately 15.8 MPa, and an impact strength of approximately 3.17 kJ/m^2) and improved thermal stabilities. The addition of sandy soil particles endowed materials with favorable flame-retarded properties, which can be resistant to fire ignition and flame out within 55 s. Moreover, the actual agriculture wastes containing mulching film residues, cotton stalk, and soil from different areas of China were also successfully transformed into functional composites, which exhibited promising mechanical, thermal, and flame-retarding properties. This study provided a simple, green, and low-cost strategy to convert agriculture mulching film wastes into functional materials, which can be recommended as a viable option to solve the problem of agriculture mulching film wastes.

Keywords: Agriculture waste; Sandy soil; Recyclability; Flame retardant; Materials

*Contact information: a: School of Agricultural Engineering and Food Science, Shandong University of Technology, Zibo, 255000, China; b: Shandong Research Center of Engineering and Technology for Clean Energy, Zibo, 255000, China; *Corresponding author: yiweiming@sdut.edu.cn*

INTRODUCTION

Plastic mulching film, one of the most commonly used materials in agricultural production, can conserve soil moisture and increase soil temperature in areas where irrigation is not available and the spring temperature is low; other benefits include higher crop yield and better crop quality (Gu *et al.* 2017; Lee *et al.* 2019; Chen *et al.* 2020; Hu *et al.* 2020). Typically, the major component of mulching film is low density and linear low-density polyethylene (Briassoulis and Schettini 2003; Kasirajan and Ngouajio 2012). This material is difficult to biodegrade due to its unique molecular structure and crystallinity, resulting in a great environmental burden (Ng *et al.* 2018). Because of the incomplete recovery after the crop season, waste mulching film debris accumulates in soil, which negatively affects the soil quality, entangles with crop roots, and inhibits the absorption of water and nutrients, thus decreasing the crop yields and limiting the sustainable development of agriculture (Liu *et al.* 2018; Qi *et al.* 2018; de Souza Machado *et al.* 2019). Moreover, such plastic residues remaining in agricultural soil can enter the ecosystem, and the microplastics may be migrated by soil organisms as carriers for other soil pollutants, or

become dust in the air, threatening the environment (Steinmetz *et al*. 2016; He *et al*. 2018). Thus, how to deal with mulching film waste in effective, green, and low-cost ways is an urgent problem needed to be solved in both agricultural production and environmental protection.

Many attempts have been made to deal with the agricultural mulching film wastes, such as the development and utilization of photodegradable or biodegradable materials, repeated use of plastics, weight reduction of mulching film, recycling, and incineration (Liu *et al.* 2014). Cyclic utilization and weight reduction of mulching film seems to be the simple way to deal with waste plastic residues. However, this strategy can only temporarily alleviate the aggravation of the problem, and collecting plastic in farmland will take a lot of time and labor. Incineration is the direct burning of agricultural residues in the field, which is another simple and direct method of waste treatment. Unfortunately, this option inevitably releases some air-borne particulates, greenhouse gas, and poses other serious consequences for the environment (Nkwachukwu *et al.* 2013; Vox *et al.* 2016). Biodegradable materials, such as mulching film, can be decomposed into small molecules after harvest season, becoming a promising strategy to reduce the pollution of the soil by plastic fragments. However, when biodegradable plastics are used in the actual environment, they often face the restriction of many environmental factors (*e.g.*, temperature, pH, or moisture) and enzymatic factors (*e.g.*, enzyme preference for plastic polymer), making the degradation of biodegradable plastics complicated and unpredictable (Lambert and Wagner 2017; Sanchez-Hernandez *et al.* 2020). Mulching film can also be turned into fuel for power plants. Although this option can protect the environment and save energy, the large amount of pollutants carried on the mulching film and the cost pressure brought by the recovery make it difficult to effectively implement the mulching film collection (Hemphill 1993).

Recently, wood-plastic composites are emerging as favorable options to recycle agriculture wastes. The concept of wood-plastic composites is straightforward: fine powder of wood, or woody biomass from agricultural residues, is blended with polymers, such as polyethylene or polypropylene, *via* extrusion, injection, or compression moulding to form simple sections, such as planks, or more complex profiles (Chan *et al.* 2017; Mohanty *et al.* 2018). Wood-plastic composites have many advanced properties, such as low moisture absorption, low density, resistance to biological attack, good dimensional stability, and a combination of high specific stiffness and strength (Sommerhuber *et al.* 2015). As a consequence, they are widely used by owners in different fields, such as different outdoor and indoor applications, like fencing, decking, railing, docks, landscaping timbers, windows, doors, and various parts of automobiles (Borah and Kim 2016). For the improvement of the material properties of wood-plastic composites, inorganic fillers, including red mud (Liu *et al.* 2016), mineral fillers (Guzel *et al.* 2016), montmorillonite (Zhu *et al.* 2019), nano-zinc oxide (Abdel-Rahman *et al.* 2020), and nano-silica (Hao *et al.* 2018; Ma *et al.* 2019), are added into the materials. For example, Vigneshwaran *et al.* (2019) used red mud and sisal fiber as fillers to reinforce unsaturated polyester resin, and the addition of red mud improved mechanical and waterproof properties of composites. Matykiewicz *et al.* (2019) added basalt powder to epoxy resin to enhance the thermomechanical properties, stiffness, and hardness of the composites. Liu *et al.* (2016) modified wood flour (WF) with sodium-montmorillonite (Na-MMT) and then compounded with polylactic acid (PLA). The physical properties, most of the mechanical properties, and thermal properties of the obtained composites were improved. Sandy soil is also an inorganic matter, and after crops were harvested, it will inevitably adhere to the

mulching film wastes and agricultural residues. Thus, an opportunity was provided to convert mulching film wastes and inorganic soil into functional wood-plastic composites with favorable strength and potential flame retarded properties, which were suitable as building materials, interior decoration, landscaping wood, doors and tables, *etc*.

Herein, cotton stalk particles-polyethylene-sandy soil composites (CS-PE-SS_x) were fabricated by simple high-speed mixing, mini-twin-screw extrusion, and micro injection molding procedures. Unlike traditional preparation of wood-plastic composites that use maleic acid polyethylene (MAPE) as compatibilizer to optimize the interface combination between hydrophobic polyethylene matrix and hydrophilic biomass (Tong *et al.* 2014; Mu *et al*. 2018), the addition of sandy soil (without MAPE) offered a procedure with easy preparation capability and relatively low cost. Due to the uniform dispersion of solid particles in the polymer matrix, the promising interface combination and the potential interacting forces between biomass and the oxygen groups on the surface of sandy soil, the resultant composites exhibited improved mechanical strength (flexural strength of approximately 29.0 MPa, tensile strength of approximately 15.8 MPa, and an impact strength of approximately 3.17 kJ/m^2). Due to the intrinsic flame-retarded properties of inorganic sandy soil and their uniform distribution in polymer matrix, the composites also showed a higher limiting oxygen index (LOI) value of 24.1% compared with 20.8% of composites without sandy soil. The composites were barely ignited by flame envelope for 10 s and exhibited flame out within 55 s. Furthermore, composites were also obtained by actual agriculture mulching film wastes from different areas of China (*e.g.*, Shandong, Jiangsu, and Xinjiang). This work may pave a simple, green, and low-cost way for the feasible management of mulching film wastes into functional flame-retarded materials.

EXPERIMENTAL

Materials

High-density polyethylene (HDPE, 9001) with a melt flow index of 0.05 g/10 min was purchased from Taiwan Plastic Co., Ltd. (Taiwan, China). Linear low-density polyethylene (LLDPE, PF0218) with a melt flow index of 2 g/10 min was bought from Xingyu Plastic Chemical Co., Ltd. (Suzhou, China). The cotton stalk (CS) was from Liaocheng, China, and crushed as particles with sizes between 80- (178 μm) and 100-mesh (125 μm). The sandy soil (SS) with a particle size less than 140-mesh (104 μm) was obtained from Liaocheng, China.

Preparation of CS-PE-SS_x Composites

The preparation procedure of CS-PE-SS_x composites is illustrated in Fig. 1. Cotton stalk powder, sandy soil, and polyethylene (the main constituent in mulching film) were chosen as main components to imitate the natural agriculture wastes (Fig. 1A). As a bio-fiber, cotton stalk mainly consists of cellulose, hemicellulose, and lignin, and the fibrous morphology and the presence of polar groups (-OH, -COOH, and other polar groups) made them promising in the fabrication of functional composites (Zheng *et al.* 2015; Yang *et al.* 2019). Moreover, sandy soil mainly consists of silicon dioxide, which was characterized of the oxygen-containing group (-OH and -O-), may exist some interacting forces with bio-fiber and facilitate the materials manufacture (Wang *et al.* 2020).

Typically, sandy soil and cotton stalk were dried at 100 °C for 24 h. Then, specific ratios (Table 1) of dried cotton stalk powder, sandy soil, HDPE, and LLDPE were mixed

in the dual-motion 3D high-speed mixer (JHN-15; Zhengzhou Jintai Metal Material Co., Ltd., Zhengzhou, China) at a speed of 15 r/min for 10 min (Fig. 1B). The mixtures were processed with the mini-twin-screw extruder (WLG10G, Shanghai Xinshuo Precision Machinery Co., Ltd., Shanghai, China) at a temperature of 180 °C and an extrusion speed of 60 r/min (Fig. 1C). Afterwards, the molten mixture was extruded into the barrel and then put into the micro injection molding machine (WZS10D, Shanghai Xinshuo Precision Machinery Co., Ltd., Shanghai, China) for injection molding (Fig. 1D). The barrel temperature was set at 180 °C, the material tube temperature was 45 °C, and the holding time was 5 s. The obtained composites were abbreviated as CS-PE-SS$_x$, where *x* represented the contents of SS in composites.

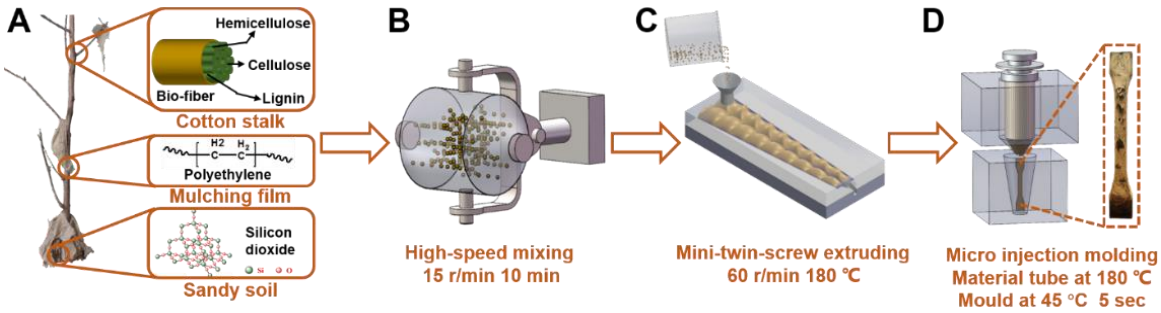

Fig. 1. Schematic synthesis of CS-PE-SS$_x$ composites: (A) photographs of cotton stalk, mulching film, and sandy soil (the brown frame emphasizes the main components of cotton stalks, polyethylene, and sandy soil); (B) High-speed mixing; (C) Mini-twin-screw extruding; (D) Micro injection molding and the photograph of CS-PE-SS$_x$ composite samples

Table 1. Contents of Different Ingredients in the Formula (wt%)

No.	1	2	3	4	5	6	7
Sandy soil	0	5	10	15	20	30	40
Cotton stalk	70	65	60	55	50	40	30
HDPE	15	15	15	15	15	15	15
LLDPE	15	15	15	15	15	15	15

Characterization

Fourier transform infrared (FT-IR) analysis was performed on a Nicolet 5700 FT-IR spectrometer (Thermo Fisher Scientific, Waltham, MA, USA) using the KBr pellet method at wavenumber range 400 to 4000 cm^{-1}. The samples were crushed into powders and washed with ethanol three times and dried at 60 °C for 24 h. The specimens for FT-IR measurement were prepared by grinding the sample solid with KBr together and then compressed into thin pellets.

X-ray diffraction (XRD) analysis was performed on a Bruker AXS D8 advance polycrystalline X-ray diffractometer (BRUKER AXS GMBH, Karlsruhe, Germany) using CuKα radiation. The operating voltage was 40 KV, the operating current was 50 mA, the sweep range was 5° to 60°, and the scanning speed was 5°/min. The samples were crushed, washed with ethanol three times, and dried at 60 °C for 24 h before XRD study.

Field emission scanning electron microscopy (FE-SEM, FEI Sirion 200; Thermo Fisher Scientific, Waltham, MA, USA) was used to characterize the surface microstructure of samples. The scanning voltage was set as 10 kV. Energy-dispersive X-ray spectroscopy mapping of broken samples was performed to verify the presence and distribution of SS in CS-PE-SS$_x$ composites.

The thermal stabilities of the samples were evaluated using a synchronous thermal analyzer (STA 449, NETZSCH Scientific Instruments Trading Ltd., Selb, Germany). The experiments were conducted in nitrogen atmosphere (20 mL/min) with the heating process from 30 °C to 1100 °C under a 10 °C/min heating rate.

Mechanical properties

The tensile and flexural properties of the samples were tested with an electronic universal testing machine (WDW1020; Changchun Kexin Co., Ltd., Changchun, China). The samples were cut into dimensions of 80 × 10 × 4 mm^3 for flexural properties testing, with a 64 mm bending span and a 5 mm/min loading speed. Samples with dimensions of 150 × 10 × 4 mm^3 were used for tensile properties tests with a 10 mm/min stretching speed. The impact performance of the samples (80 × 10 × 4 mm^3) was tested using a pendulum electronic impact tester (JB-300b; Jinan Hengsi Shengda Instrument Co., Ltd., Jinan, China) under an impact energy of 1 J. All the mechanical properties tests were processed for more than five replicates and averaged for each test.

Flame-retarded properties

The flame-retardant properties of samples were studied by evaluating their combustion processes. Typically, on one hand, the CS-PE-SS_x samples (20 × 10 × 4 mm^3) with different SS contents were ignited by flame envelope for 10 s, and their burning status and flame sizes were recorded. On the other hand, the CS-PE-SS_x samples (25 × 10 × 4 mm^3) with different SS contents were ignited and kept burning in the air, and their flame out time and burning extents were recorded. An intelligent oxygen index analyzer (ZR-01; Qingdao Shan Fang Instrument Co., Ltd., Qingdao, China) was used to measure the LOI values of CS-PE-SS_x composites. The dimensions of samples were 80 × 10 × 4 mm^3 and the mixed gas flow rate was 40 ± 2 mm/s. The LOI values and corresponding estimated standard deviation were calculated according to Eq. 1,

$$OI = C_f + kd \quad (1)$$

where *OI* represents the limiting oxygen index (vol%), C_f is the last oxygen concentration value (vol%) of each group of measurements, *d* represents the difference of the oxygen concentration of each measurement (vol%), and *k* is obtained by comparing the last six measurements to find the standard. The value of *d* can be optimized according to Eqs. 2 and 3,

$$\hat{\sigma} = \left[\frac{\sum_{i=1}^{n}(c_i - OI)^2}{n-1}\right]^{1/2} \quad (2)$$

$$\frac{2\hat{\sigma}}{3} < d < 1.5\hat{\sigma} \quad (3)$$

where σ represents the standard deviation, c_i is the oxygen concentration (vol%) obtained from the last six measurements of each group, and *n* is the number of measurements of the oxygen concentration. If $d < (2\sigma) / 3$, then increase the value of *d* and repeat the experiment until the condition is met. If $d > 1.5\sigma$, then decrease the value of *d* and repeat the experiment.

RESULTS AND DISCUSSION

FT-IR

The FT-IR analysis was carried out on SS, LLDPE, CS, and CS-PE-SS$_x$ with different SS contents (Fig. 2). For cotton stalk, the bands at 3419 cm^{-1}, 2918 cm^{-1} and 2850 cm^{-1}, 1743 cm^{-1}, 1633 cm^{-1}, 1510 cm^{-1} and 1455 cm^{-1}, 1426 cm^{-1} and 1375 cm^{-1}, were attributed to the hydrogen bonded O-H stretching vibration, C-H stretching vibration from -CH and -CH$_2$ in cellulose and hemicellulose components, C=O valance vibration of hemicellulose acetyl group or ester linkage of carboxylic group of feruli and *p*-coumeric acid in lignin, the vibration of C=O stretch of conjugated p-substituted aryl ketones, the -C=C- stretch of the aromatic rings of lignin, and -CH, -CH$_2$ vibrations and aromatic ring modes, respectively (Fig. 2A) (Rahbar Shamskar *et al.* 2016). However, the characteristic peak at 1743 cm^{-1} and 1633 cm^{-1} exhibited blue shifts to 1735 cm^{-1} and 1624 cm^{-1} of CS-PE-SS$_{40}$, indicating the changes of their chemical environment, which was triggered by the possible interactions between components in CS-PE-SS$_{40}$ (Fig. 2B). The main component of sandy soil was silicon dioxide. The polar groups on the surface of silicon dioxide may contribute some interacting forces with biomass, resulting in the shift of the characteristic peaks in the FT-IR spectrum (Boehm 1966). Thus, the interaction between CS and SS indicated promising combination among components, mechanical properties, and functionalities.

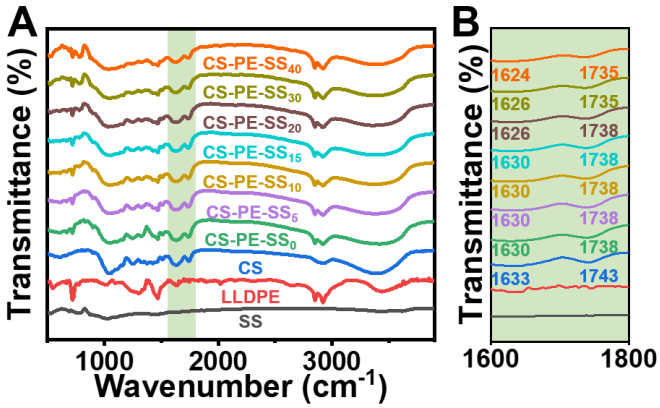

Fig. 2. (A) The FT-IR spectra of CS, SS, LLDPE, and CS-PE-SS$_x$ composites with different SS contents; (B) The amplified FT-IR spectra at wavenumber 1600 to 1800 cm^{-1}, emphasizing the blue shift of wavenumber

XRD

The XRD patterns of CS, HDPE, SS, and CS-PE-SS$_{40}$ are shown in Fig. 3. The CS showed two regions with peak values of approximately 16.9° and 22.1°, demonstrated an amorphous state and cellulose I, respectively (Zhou *et al.* 2020). Two main diffraction peaks of the HDPE could be observed at 21.6° and 24°, which corresponded to (110) and (200) crystal planes (Zhang *et al.* 2019). The sandy soil displayed two strong diffraction peaks at 20.9° and 26.7°, which were assigned to the (100) and (101) crystal planes (Vijay *et al.* 2019). Similarly, CS-PE-SS$_{40}$ composites exhibited the characteristic peaks of HDPE, SS, and CS, implying that the crystal structures of each component were not changed during the preparation procedure. The retainment of intrinsic properties of each component in CS-PE-SS$_x$ composites indicated that this materials preparation was feasible and non-destructive, which was promising in further applications such as flame retard.

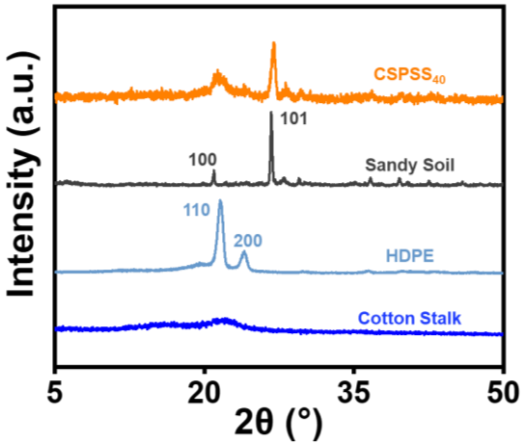

Fig. 3. XRD curves of HDPE, sandy soil, cotton stalk, and CS-PE-SS$_{40}$

SEM

Figure 4A through 4H showed the cross-section SEM images of CS-PE-SS$_{0\text{-}40}$. Composites without SS exhibited that cotton stalk particles that were well combined with polyethylene matrix (Fig. 4A).

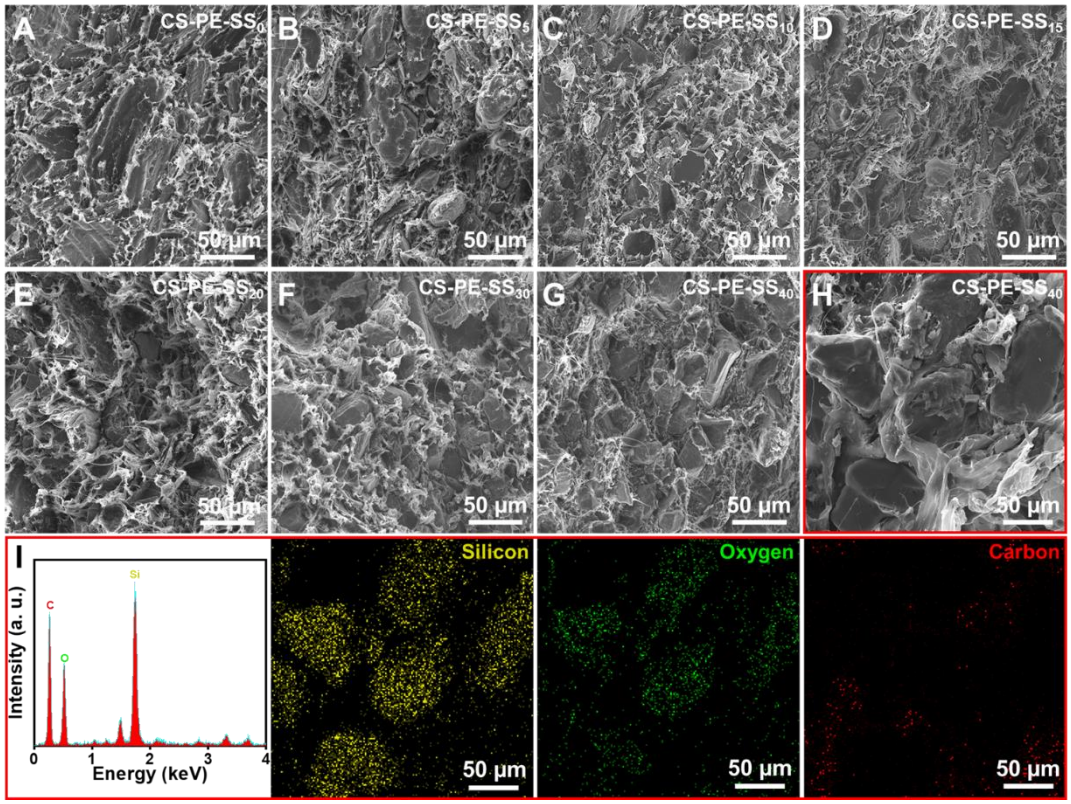

Fig. 4. Scanning electron micrographs of composites with different sandy soil contents (A through G); SEM image of sandy soil 40 wt% (H), EDS and mapping of silicon, oxygen, and carbon (I)

After adding SS, inorganic particles with diameters ranging from 10 μm to 110 μm were observed. The distribution of SS in polyethylene matrix became dense and uniform

as their contents increased, indicating favorable adhesion of polyethylene on the surfaces of SS (Fig. 4B through 4G). In the amplified SEM image of CS-PE-SS_{40} composites, melt polymer matrix as fluid at high temperature tightly attached onto the surfaces of SS after cooling and showed no obvious cracks (Fig. 4H) (Essabir *et al.* 2017; Spoerk *et al.* 2017). The corresponding energy-dispersive X-ray spectrum and mapping further implied the presence and uniform distribution of SS in CS-PE-SS_{40} composites (Fig. 4I). The favorable combination in the interfaces and potential interactions between components were critical for the performance of functional composites. Thus, the well dispersion of SS in polymer matrix combined with the tight interface adhesion and interactions between SS and CS particles exhibited promising potential in the development of mechanical properties and thermal stabilities of CS-PE-SS_{40} composites.

Mechanical Properties of CS-PE-SS_x

To study the impact of SS on the mechanical properties of CS-PE-SS_x composites, the flexural strength, tensile strength, and impact strength of CS-PE-SS_0, CS-PE-SS_{10}, CS-PE-SS_{20}, CS-PE-SS_{30}, and CS-PE-SS_{40} composites were tested (Fig. 5). The mechanical strength, such as flexural strength, tensile strength, and impact strength, increased with more SS addition and reached values of 29.0 MPa, 15.8 MPa, and 3.17 kJ/m^2 for CS-PE-SS_{40} composites, respectively (Figs. 5A through 5C). The improvement of mechanical properties of composites may be attributed to three reasons. Firstly, SS particles with high stiffness were well distributed in polymer matrix. They transferred stress efficiently and thus improved the mechanical properties of CS-PE-SS_x composites (Chan *et al.* 2019). Secondly, the rigid SS particles embedded in polymer matrix may form a concentration of force when external forces were applied, thereby inducing crazing in the interface between SS and polyethylene matrix. Inorganic particles can prevent the development of crazing, and the increase of SS contents inhibits the growth of the number of crazing and improves the strength of the composites (Keskisaari *et al.* 2016). Lastly, the interacting forces between SS particles and CS powders also endowed composites favorable resistance to external forces and thus improved their mechanical properties. Overall, the composites fabricated with SS, CS, and PE were mechanically strong and suitable for functional wood-plastic plate materials.

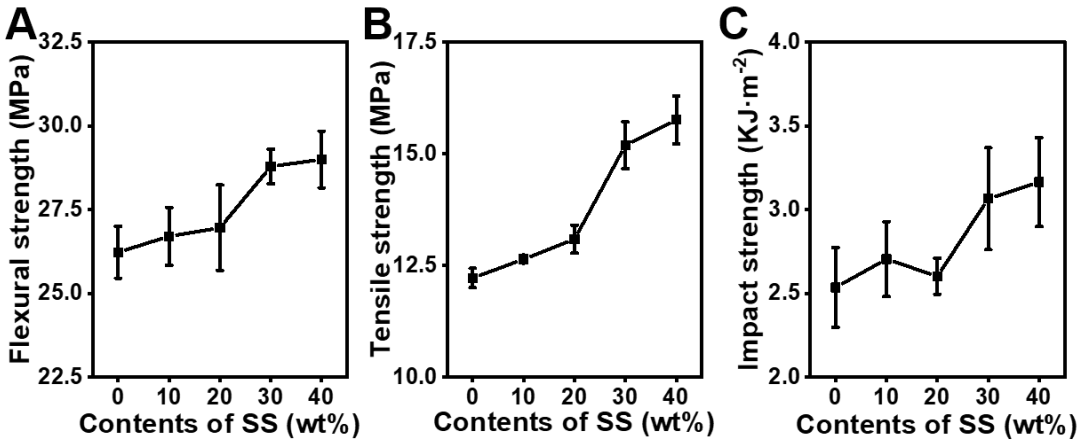

Fig. 5. (A through C) Flexural strength, tensile strength, and impact strength, respectively, of composites with different sandy soil contents

Thermal Properties of CS-PE-SS$_x$

The mass loss curves and mass loss derivatives of HDPE, LLDPE, CS, SS, CS-PE-SS$_0$, CS-PE-SS$_5$, CS-PE-SS$_{10}$, CS-PE-SS$_{15}$, CS-PE-SS$_{20}$, CS-PE-SS$_{30}$, and CS-PE-SS$_{40}$ composites are presented in Fig. 6 to evaluate the effect of SS on the thermal stabilities of CS-PE-SS$_x$ composites. Both HDPE and LLDPE presented only one major step of thermal decomposition. The steps around 500 °C of HDPE and LLDPE were related to the break of carbon-carbon bond of the polymeric chains and formation of volatiles compounds (Moreno and Saron 2017). The main weight loss process of CS was around 350 °C, leading to 55% of weight loss, which was mainly caused by thermal depolymerization of the hemicellulose, breaking of glycosidic bond of the cellulose, and decomposition of the *α*-cellulose. Lignin in CS also started decomposition at approximately 500 °C (Guo *et al.* 2020). However, the thermogravimetric curve of SS exhibited only a weak peak between 630 °C and 770 °C, which can be attributed to the degradation of $CaCO_3$ into CaO. It was noteworthy that CS-PE-SS$_x$ composites showed less mass loss compared with pure CS, HDPE, LDPE, and composites without SS. This may be due to the high thermal stability of SS and strong interacting forces with CS and fine dispersion in polymer matrix, which can prevent the penetration of volatile degradation products from the composites (Subramani *et al.* 2007; Koohestani *et al.* 2017). Furthermore, the temperature at 10% weight loss of CS-PE-SS$_x$ composites also increased from 252 °C of CS to 312 °C of CS-PE-SS$_{40}$. All the results provided good evidence that the thermal stabilities of the composites were enhanced effectively.

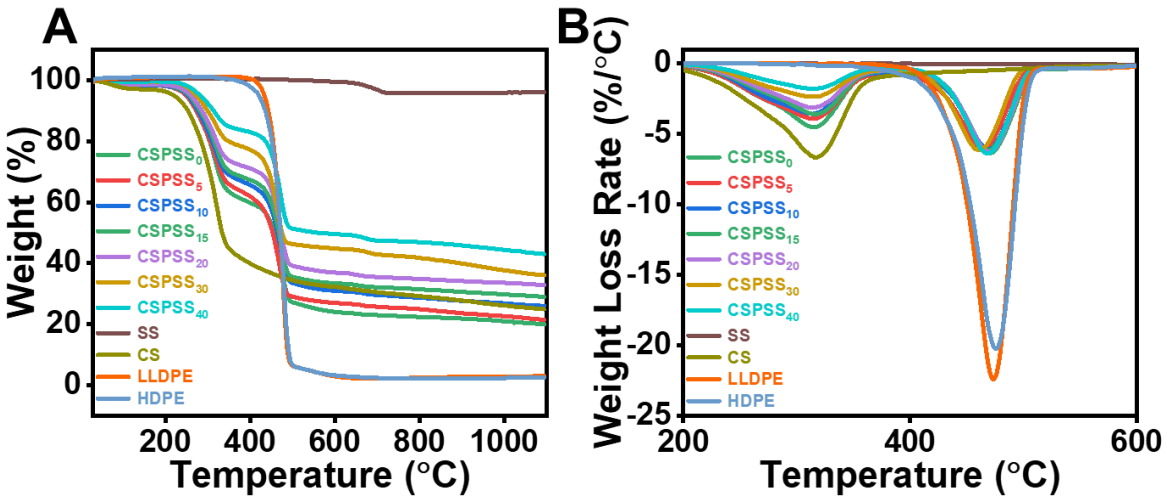

Fig. 6. TG (A) and DTG (B) curves of SS, CS, LLDPE, HDPE, and CS-PE-SS$_x$ composites; the contents of SS were 0 wt%, 5 wt%, 10 wt%, 15 wt%, 20 wt%, 30 wt%, and 40 wt%, respectively.

Flame Retardant Properties of CS-PE-SS$_x$

The SS, as an inorganic flame retardant, can effectively weaken the transfer of heat and the volatilization of combustible gas and reduce the contact area between combustible and air, making it difficult for the flame to continue to burn down, and finally improving the flame-retardant properties of the composites (Schirp and Su 2016; Zhang *et al.* 2017). In Fig. 7A, composites with different SS contents were ignited by flame lighter. It can be observed that when the composite sample only contained cotton stalk and polymer matrix, the flame became very bright after 10 s of ignition. While the composites with SS addition, it was difficult to ignite. Additionally, with the increase of SS contents, the flame intensity

decreased obviously and was even unignited for CS-PE-SS$_{40}$. The flame out time and burning distance were recorded after the tops of the samples were fully ignited (Fig. 7B through 7D). When the contents of SS were 0 wt%, the sample showed sustained combustion until it burned out. However, with the addition of SS, the samples exhibited obvious extinguishment phenomenon and the extinguishment time rapidly decreased (CS-PE-SS$_{40}$ composites flamed out within 55 s). Compared with the composites without SS, the burning distance of the samples contained SS was remarkably shortened and an almost 75% decrease occurred with only 5 wt% SS addition.

The LOI value corresponds to the oxygen content required for combustion to occur, and a high limiting oxygen index value means high flame-retarded properties. (Zhou and Fu 2020). The LOI values of the composites were shown in Fig. 7E. When the proportion of SS was 0 wt%, the LOI values of the composite was 20.8%. The LOI values of the composites increased gradually with more SS usage. When the proportion of SS reached 40 wt%, the LOI value of the composite reached 24.1%. Many flame retardants, such as aluminum hydrogen phosphonate, triphenyl phosphate, ammonium polyphosphate, and so on, were applied to improve the flame-retardant abilities of wood-plastic composites, and their LOI values were calculated between approximately 18.1% and 26.6% (Altun *et al.* 2016; Pham *et al.* 2019; Yin *et al.* 2019). Thus, the CS-PE-SS$_x$ composites obtained from agricultural mulching film wastes were judged to be suitable for flame retard applications.

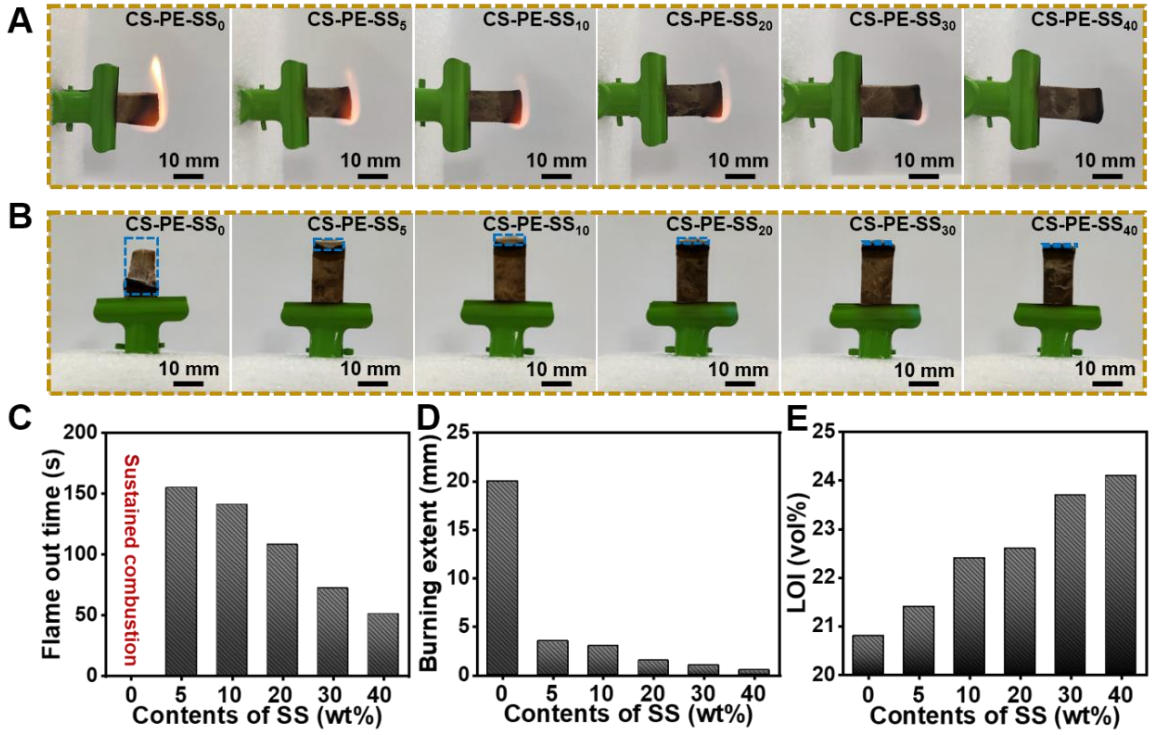

Fig. 7. The 10 s ignition test of the specimen (A), burning distance tests of the specimen (B), diagram of flame out time (C), diagram of burning extent (D), and LOI values of composites samples (E)

Feasibility Evaluation of the Materials Fabrication

To evaluate the feasibility of the authors' management on agricultural wastes, soil from Xinjiang, Shandong, and Jiangsu were selected to composite with waste mulching film and cotton stalk. The results showed that all the agricultural wastes used can form

intact composites with promising properties (Fig. 8A). The flexural strength, tensile strength, and impact strength of the three composites were relatively lower than the commercial wood-plastic composites, but still suitable for applications in plates fields (Hyvärinen *et al.* 2014). The LOI values of the composites with different soil from three regions were approximately 23.5%, which was higher than that of the sample without soil. These results indicated that the conversion of agricultural wastes into flame retardant materials was feasible, and the waste soil acts as a flame retardant in the composites was of noticeable importance for the authors to develop an efficient and economical strategy to utilize the waste resources.

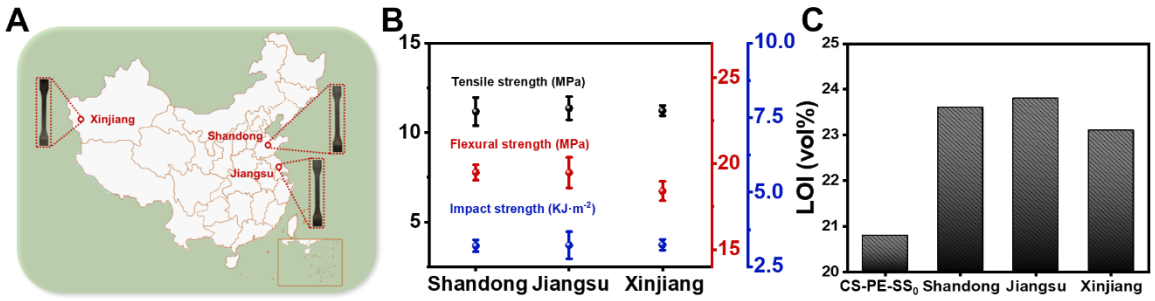

Fig. 8. (A) Soil acquired in different provinces of China and the photographs of corresponding composites; (B) Mechanical properties; and (C) LOI values of the composites fabricated using agricultural mulching film wastes from Shandong, Jiangsu, and Xinjiang province of China

CONCLUSIONS

1. Simple compounding and injection molding procedures were applied to convert plastic agriculture mulching film wastes into functional flame-retarded composites directly. The added sandy soil particles were uniformly dispersed in the polymer matrix and showed promising interface combination.
2. The resultant composites showed a flexural strength of approximately 29.0 MPa, a tensile strength approximately 15.8 MPa, an impact strength of approximately 3.17 kJ/m^2 and improved thermal stabilities.
3. The addition of sandy soil particles endowed materials favorable flame-retarded properties, which can resistant to fire ignition and flame out within 55 s.

ACKNOWLEDGMENTS

The authors are grateful for the support of the financial support of the National Key Research and Development Program of China (No. 2018YFD1101001); the distinguished expert of Taishan scholars Shandong province project and the higher education superior discipline team training program of Shandong province.

REFERENCES CITED

Abdel-Rahman, H. A., Awad, E. H., and Fathy, R. M. (2020). "Effect of modified nano zinc oxide on physico-chemical and antimicrobial properties of gamma-irradiated sawdust/epoxy composites," *J. Compos. Mater.* 54(3), 331-343. DOI: 10.1177/0021998319863835

Altun, Y., Doğan, M., and Bayramlı, E. (2016). "Flammability and thermal degradation behavior of flame retardant treated wood flour containing intumescent LDPE composites," *Eur. J. Wood Wood Prod.* 74, 851-856. DOI: 10.1007/s00107-016-1042-1

Boehm, H. P. (1966). "Functional groups on the surfaces of solids," *Angew. Chem. Int. Ed. Engl.* 5(6), 533-544. DOI: 10.1002/anie.196605331

Borah, J. S., and Kim, D. S. (2016). "Recent development in thermoplastic/wood composites and nanocomposites: A review," *Korean J. Chem. Eng.* 33, 3035-3049. DOI: 10.1007/s11814-016-0183-6

Briassoulis, D., and Schettini, E. (2003). "Analysis and design of low-density polyethylene greenhouse films," *Biosyst. Eng.* 84(3), 303-314. DOI: 10.1016/S1537-5110(02)00241-6

Chan, C. M., Vandi, L., Pratt, S., Halley, P., Richardson, D., Werker, A., and Laycock, B. (2017). "Composites of wood and biodegradable thermoplastics: A review," *Polym. Rev.* 58(3), 444-494. DOI: 10.1080/15583724.2017.1380039

Chan, J. X., Wong, J. F., Hassan, A., Mohamad, Z., and Othman, N. (2019). "Mechanical properties of wollastonite reinforced thermoplastic composites: A review," *Polym. Composite.* 41(2), 395-429. DOI: 10.1002/pc.25403

Chen, N., Li, X., Šimůnek, J., Shi, H., Ding, Z., and Zhang, Y. (2020). "The effects of biodegradable and plastic film mulching on nitrogen uptake, distribution, and leaching in a drip-irrigated sandy field," *Agric. Ecosyst. Environ.* 292, Article ID 106817. DOI: 10.1016/j.agee.2020.106817

de Souza Machado, A. A., Lau, C. W., Kloas, W., Bergmann, J., Bachelier, J. B., Faltin, E., Becker, R., Görlich, A. S., and Rillig, M. C. (2019). "Microplastics can change soil properties and affect plant performance," *Environ. Sci. Technol.* 53(10), 6044-6052. DOI: 10.1021/acs.est.9b01339

Essabir, H., Bensalah, M. O., Rodrigue, D., Bouhfid, R., and Qaiss, A. E. K. (2017). "A comparison between bio- and mineral calcium carbonate on the properties of polypropylene composites," *Constr. Build. Mater.* 134, 549-555. DOI: 10.1016/j.conbuildmat.2016.12.199

Gu, X., Li, Y., and Du, Y. (2017). "Biodegradable film mulching improves soil temperature, moisture and seed yield of winter oilseed rape (*Brassica napus* L.)," *Soil Tillage Res.* 171, 42-50. DOI: 10.1016/j.still.2017.04.008

Guo, Y., Wang, L., Wang, H., Chen, Y., Zhu, S., Chen, T., and Luo, P. (2020). "Properties of bamboo flour/high-density polyethylene composites reinforced with ultrahigh molecular weight polyethylene," *J. Appl. Polym. Sci.* 137(33), Article ID 48971. DOI: 10.1002/app.48971

Guzel, G., Sivrikaya, O., and Deveci, H. (2016). "The use of colemanite and ulexite as novel fillers in epoxy composites: Influences on thermal and physico-mechanical properties," *Compos. Part B- Eng.* 100, 1-9. DOI: 10.1016/j.compositesb.2016.06.054

Hao, X., Zhou, H., Xie, Y., Xiao, Z., Wang, H., and Wang, Q. (2018). "Mechanical reinforcement and creep resistance of coextruded wood flour/polyethylene

composites by shell-layer treatment with nano - and micro-SiO_2 particles," *Polym. Compos.* 40(4), 1576-1584. DOI: 10.1002/pc.24901

Hemphill, D. D. J. (1993). "Agricultural plastics as solid waste: What are the options for disposal?," *HortTechnology* 3(1), 70-73. DOI: 10.21273/HORTTECH.3.1.70

He, D., Luo, Y., Lu, S., Liu, M., Song, Y., and Lei, L. (2018). "Microplastics in soils: Analytical methods, pollution characteristics and ecological risks," *TrAC, Trends Anal. Chem.* 109, 163-172. DOI: 10.1016/j.trac.2018.10.006

Hu, Q., Li, X., Gonçalves, J. M., Shi, H., Tian, T., and Chen, N. (2020). "Effects of residual plastic-film mulch on field corn growth and productivity," *Sci. Total Environ.* 729, Article ID 138901. DOI: 10.1016/j.scitotenv.2020.138901

Hyvärinen, M., Paajanen, J., and Kärki, T. (2014). "Determination and comparison of material properties of commercial wood-plastic composite products," *Adv. Mater. Res.* 1051, 242-249. DOI: 10.4028/www.scientific.net/AMR.1051.242

Kasirajan, S., and Ngouajio, M. (2012). "Polyethylene and biodegradable mulches for agricultural applications: A review," *Agron. Sustainable Dev.* 33, 443. DOI: 10.1007/s13593-012-0132-7

Keskisaari, A., Butylina, S., and Kärki, T. (2016). "Use of construction and demolition wastes as mineral fillers in hybrid wood-polymer composites," *J. Appl. Polym. Sci.* 133(19), Article ID 43412. DOI: 10.1002/app.43412

Koohestani, B., Ganetri, I., and Yilmaz, E. (2017). "Effects of silane modified minerals on mechanical, microstructural, thermal, and rheological properties of wood plastic composites," *Compos. Part B- Eng.* 111, 103-111. DOI: 10.1016/j.compositesb.2016.12.021

Lambert, S., and Wagner, M. (2017). "Environmental performance of bio-based and biodegradable plastics: The road ahead," *Chem. Soc. Rev.* 46(22), 6855-6871. DOI: 10.1039/C7CS00149E

Lee, J. G., Cho, S. R., Jeong, S. T., Hwang, H. Y., and Kim, P. J. (2019). "Different response of plastic film mulching on greenhouse gas intensity (GHGI) between chemical and organic fertilization in maize upland soil," *Sci. Total Environ.* 696, Article ID 133827. DOI: 10.1016/j.scitotenv.2019.133827

Liu, E. K., He, W. Q., and Yan, C. R. (2014). "'White revolution' to 'white pollution'-agricultural plastic film mulch in China," *Environ. Res. Lett.* 9(9), Article ID 091001. DOI: 10.1088/1748-9326/9/9/091001

Liu, L., Zhang, Y., Lv, F., Yang, B., and Meng, X. (2016a). "Effects of red mud on rheological, crystalline, and mechanical properties of red mud/PBAT composites," *Polym. Compos.* 37(7), 2001-2007. DOI: 10.1002/pc.23378

Liu, R., Chen, Y., and Cao, J. (2016b). "Effects of modifier type on properties of *in situ* organo-montmorillonite modified wood flour/poly (lactic acid) composites," *ACS Appl. Mater. Interfaces.* 8(1), 161-168. DOI: 10.1021/acsami.5b07989

Liu, M., Lu, S., Song, Y., Lei, L., Hu, J., Lv, W., Zhou, W., Cao, C., Shi, H., Yang, X., and He, D. (2018). "Microplastic and mesoplastic pollution in farmland soils in suburbs of Shanghai, China," *Environ. Pollut.* 242(Part A), 855-862. DOI: 10.1016/j.envpol.2018.07.051

Ma, Y., He, H., Huang, B., Jing, H., and Zhao, Z. (2019). "*In situ* fabrication of wood flour/nano silica hybrid and its application in polypropylene-based wood-plastic composites," *Polym. Compos.* 41(2), 573-584. DOI: 10.1002/pc.25389

Matykiewicz, D., Barczewski, M., and Michałowski, S. (2019). "Basalt powder as an eco-friendly filler for epoxy composites: Thermal and thermo-mechanical properties

assessment," *Compos. Part B- Eng.* 164, 272-279. DOI: 10.1016/j.compositesb.2018.11.073

Mohanty, A. K., Vivekanandhan, S., Pin, J. M., and Misra, M. (2018). "Composites from renewable and sustainable resources: Challenges and innovations," *Science* 362(6414), 536-542. DOI: 10.1126/science.aat9072

Moreno, D. D. P., and Saron, C. (2017). "Low-density polyethylene waste/recycled wood composites," *Compos. Struct.* 176, 1152-1157. DOI: 10.1016/j.compstruct.2017.05.076

Mu, B., Wang, H., Hao, X., and Wang, Q. (2018). "Morphology, mechanical properties and dimensional stability of biomass particles/high density polyethylene composites: Effect of species and composition," *Polymers* 10, Article number 308. DOI: 10.3390/polym10030308

Ng, E., Huerta Lwanga, E., Eldridge, S. M., Johnston, P., Hu, H., Geissen, V., and Chen, D. (2018). "An overview of microplastic and nanoplastic pollution in agroecosystems," *Sci. Total Environ.* 627, 1377-1388. DOI: 10.1016/j.scitotenv.2018.01.341

Nkwachukwu, O., Chima, C., Ikenna, A., and Albert, L. (2013). "Focus on potential environmental issues on plastic world towards a sustainable plastic recycling in developing countries," *Int. J. Ind. Chem.* 4, Article number 34. DOI: 10.1186/2228-5547-4-34

Pham, L. H., Nguyen, H. D., Kim, J., and Hoang, D. (2019). "Thermal properties and fire retardancy of polypropylene/wood flour composites containing eco-friendly flame retardants," *Fibers Polym.* 20, 2383-2389. DOI: 10.1007/s12221-019-1179-8

Qi, Y., Yang, X., Pelaez, A. M., Huerta Lwanga, E., Beriot, N., Gertsen, H., Garbeva, P., and Geissen, V. (2018). "Macro- and micro- plastics in soil-plant system: Effects of plastic mulch film residues on wheat (*Triticum aestivum*) growth," *Sci. Total Environ.* 645, 1048-1056. DOI: 10.1016/j.scitotenv.2018.07.229

Rahbar Shamskar, K., Heidari, H., and Rashidi, A. (2016). "Preparation and evaluation of nanocrystalline cellulose aerogels from raw cotton and cotton stalk," *Ind. Crop. Prod.* 93, 203-211. DOI: 10.1016/j.indcrop.2016.01.044

Sanchez-Hernandez, J. C., Capowiez, Y., and Ro, K. S. (2020). "Potential use of earthworms to enhance decaying of biodegradable plastics," *ACS Sustain. Chem. Eng.* 8(11), 4292-4316. DOI: 10.1021/acssuschemeng.9b05450

Schirp, A., and Su, S. (2016). "Effectiveness of pre-treated wood particles and halogen-free flame retardants used in wood-plastic composites," *Polym. Degrad. Stabil.* 126, 81-92. DOI: 10.1016/j.polymdegradstab.2016.01.016

Sommerhuber, P. F., Welling, J., and Krause, A. (2015). "Substitution potentials of recycled HDPE and wood particles from post-consumer packaging waste in wood-plastic composites," *Waste. Manage.* 46, 76-85. DOI: 10.1016/j.wasman.2015.09.011

Spoerk, M., Sapkota, J., Weingrill, G., Fischinger, T., Arbeiter, F., and Holzer, C. (2017). "Shrinkage and warpage optimization of expanded-perlite-filled polypropylene composites in extrusion-based additive manufacturing," *Macromol. Mater. Eng.* 302(10), Article ID 1700143. DOI: 10.1002/mame.201700143

Steinmetz, Z., Wollmann, C., Schaefer, M., Buchmann, C., David, J., Tröger, J., Muñoza, K., Frörd, O., and Schaumannet, G. E. (2016). "Plastic mulching in agriculture. Trading short-term agronomic benefits for long-term soil degradation?," *Sci. Total Environ.* 550, 690-705. DOI: 10.1016/j.scitotenv.2016.01.153

Subramani, S., Lee, J. Y., Kim, J. H., and Cheong, I. W. (2007). "Crosslinked aqueous dispersion of silylated poly (urethane–urea)/clay nanocomposites," *Compos. Sci. Technol.* 67(7-8), 1561-1573. DOI: 10.1016/j.compscitech.2006.07.011

Tong, J., Royan, N. R., Ng, Y. C., Ab Ghani, M. H., and Ahmad, S. (2014). "Study of the mechanical and morphology properties of recycled HDPE composite using rice husk filler," *Adv. Mater. Sci. Eng.* 2014, 1-06. DOI: 10.3390/polym10030308

Vigneshwaran, S., Uthayakumar, M., and Arumugaprabu, V. (2019). "Development and sustainability of industrial waste-based red mud hybrid composites," *J. Clean. Prod.* 230, 862-868. DOI: 10.1016/j.jclepro.2019.05.131

Vijay, R., Lenin Singaravelu, D., Vinod, A., Sanjay, M. R., Siengchin, S., Jawaid, M., Khane, A., and Parameswaranpillai, J. (2019). "Characterization of raw and alkali treated new natural cellulosic fibers from *Tridax procumbens*," *Int. J. Biol. Macromol.* 125, 99-108. DOI: 10.1016/j.ijbiomac.2018.12.056

Vox, G., Loisi, R. V., Blanco, I., Mugnozza, G. S., and Schettini, E. (2016). "Mapping of agriculture plastic waste," *Agric. Agric. Sci. Procedia* 8, 583-591. DOI: 10.1016/j.aaspro.2016.02.080

Wang, C., Cai, Z., Wang, T., and Chen, K. (2020). "Preparation and thermal properties of shape-stabilized 1, 8-octanediol /SiO_2 composites *via* sol gel methods," *Mater. Chem. Phys.* 250, Article ID 123041. DOI: 10.1016/j.matchemphys.2020.123041

Yang, J., Ching, Y., and Chuah, C. (2019). "Applications of lignocellulosic fibers and lignin in bioplastics: A review," *Polymers* 11(5), Article number 751. DOI: 10.3390/polym11050751

Yin, H., Sypaseuth, F. D., Schubert, M., Schoch, R., Bastian, M., and Schartel, B. (2019). "Routes to halogen-free flame-retardant polypropylene wood plastic composites," *Polym. Adv. Technol.* 30(1), 187-202. DOI: 10.1002/pat.4458

Zhang, Q., Cai, H., Yang, K., and Yi, W. (2017). "Effect of biochar on mechanical and flame retardant properties of wood - Plastic composites," *Results Phys.* 7, 2391-2395. DOI: 10.1016/j.rinp.2017.04.025

Zhang, Q., Khan, M. U., Lin, X., Cai, H., and Lei, H. (2019). "Temperature varied biochar as a reinforcing filler for high-density polyethylene composites," *Compos. Part B- Eng.* 175, Article ID 107151. DOI: 10.1016/j.compositesb.2019.107151

Zheng, A., Jiang, L., Zhao, Z., Huang, Z., Zhao, K., Wei, G., Wang, X., He, F., and Li, H. (2015). "Impact of torrefaction on the chemical structure and catalytic fast pyrolysis behavior of hemicellulose, lignin, and cellulose," *Energ. Fuels* 29(12), 8027-8034. DOI: 10.1021/acs.energyfuels.5b01765

Zhou, L., and Fu, Y. (2020). "Flame-retardant wood composites based on immobilizing with chitosan/sodium phytate/nano-TiO_2-ZnO coatings *via* layer-by-layer self-assembly," *Coatings* 10(3), Article number 296. DOI: 10.3390/coatings10030296

Zhou, B., Wang, L., Ma, G., Zhao, X., and Zhao, X. (2020). "Preparation and properties of bio-geopolymer composites with waste cotton stalk materials," *J. Clean. Prod.* 245, Article ID 118842. DOI: 10.1016/j.jclepro.2019.118842

Zhu, T. T., Zhou, C. H., Kabwe, F. B., Wu, Q. Q., Li, C. S., and Zhang, J. R. (2019). "Exfoliation of montmorillonite and related properties of clay/polymer nanocomposites," *Appl. Clay Sci.* 169, 48-66. DOI: 10.1016/j.clay.2018.12.006

Article submitted: November 10, 2020; Peer review completed: February 6, 2021; Revised version received and accepted; February 21, 2021; Published: February 26, 2021.
DOI: 10.15376/biores.16.2.2838-2852